OEM4 Inertial: An Inertial/GPS Navigation System on the OEM4 Receiver

Tom Ford, NovAtel Inc., 1120-68th Ave., N.E., Calgary, Alberta, T2E 8S5,   tford@novatel.ca
Janet Neumann, NovAtel Inc., 1120-68th Ave., N.E., Calgary, Alberta, T2E 8S5, jneumann@novatel.ca
Mike Bobye, NovAtel Inc., 1120-68th Ave., N.E., Calgary, Alberta, T2E 8S5, mbobye@novatel.ca

BIOGRAPHIES

Tom Ford is a GPS specialist at NovAtel Inc.. He has a BMath degree from the University of Waterloo (1975) and a BSc in survey science from the University of Toronto (1981). He did research in the inertial and GPS field at Sheltech and Nortech surveys before becoming a member of the original group of GPS developers for NovAtel Communications (now NovAtel Inc.). He has helped develop many of the core tracking, positioning and attitude determination technologies at NovAtel Inc Over the past few years his focus has been to develop and implement inertial/GPS algorithms for an integrated INS/GPS system. In addition he has been developing specific GPS only positioning methods for other applications.

Janet Brown Neumann obtained a BSEE from the University of Kansas in 1978 and an MSEE from Iowa State University in 1981. She has been active in many different areas of GPS software and algorithm development since 1983, with her recent focus being on carrier phase positioning methods and software and integration of GPS with other positioning methods. She has been working in the NovAtel GPS group since 1990.

Mike Bobye is a member of the GPS research group at NovAtel Inc. where he has worked as an applications engineer since graduating with a BSc in Geomatics Engineering from the University of Calgary in 2000.

ABSTRACT

Inertial integration with various systems has been investigated since the inception of inertial navigation devices more than 50 years ago. A natural integration for an inertial system is GPS, and this type of coupling has been investigated for the last 20 years since GPS was developed. Two years ago, NovAtel Inc. began to develop a prototype of such an integrated system. The components of the prototype system were a Honeywell HG1700 IMU and first an OEM3 followed by an OEM4 GPS receiver. The objective of the development was to provide a tightly integrated system at reasonable cost, which could give positioning continuously at a 10 cm level provided the GPS signal outages were of short duration. The approach taken during the system development was to take advantage of the existing GPS navigation algorithms and supplement these with a set of modified inertial algorithms taken from a software suite (Kingspad) provided by the University of Calgary and to use these in a decentralised process that could run on the target processor on the OEM4 board. The result of this development is a modular system, which fulfils the accuracy requirements noted and resides entirely on the OEM4 receiver.

During the system development, investigations into the observability of system components were made. In an inertial system, the measurements of the system are used to provide the coefficients of the differential equation set which describes the dynamics of the system errors. Noise on these measurements tricks the Kalman filter into a condition of "false observability". This condition was investigated and a solution to this problem was implemented. In addition, modelling approaches related to the HG1700 were investigated and implemented. Finally, the feedback to the GPS filter to aid its resolution was investigated and this was implemented.

In this paper, the authors propose to describe the system architecture, the particulars of the system development noted above and to provide test results, which demonstrates the system performance in various environments.

INTRODUCTION

In areas where the satellite coverage is restricted for short periods of time, a serious shortcoming of a GPS only system in the unavailability of position and velocity data during those periods. In addition, the lack of GPS satellites for short periods of time can cause a serious degradation in the type of position information available even when satellites are visible. If the periods of visibility are too short, then the system will loose RTK availability entirely. For some applications the lack of accurate and continuous position information precludes the use of GPS as a navigation tool.

In late 1998 NovAtel Inc. identified an opportunity to improve the navigation capabilities of a GPS only system by supplementing it with some kind of medium grade inertial unit. The idea of the supplementary system was to bridge gaps in GPS coverage, and to seed the resolution process in the RTK filter in order to help the filter resolve ambiguities faster.

The initial approach was to use an OEM 3 (Millennium™) GPS receiver from NovAtel Inc. and an HG1700 AG11 strapdown inertial unit from Honeywell and run the inertial

processing software on the NovAtel Inc PDC (data collector card) as a development platform until the OEM 4 receiver was ready. However, the PDC card did not have enough throughput to reliably process the inertial data, so the PDC based prototype never did work properly. Instead, the PDC card became a data collection and time synchronisation unit and the processing software was developed on an offline platform until the final processing target, the OEM 4 was ready. The offline development program which resulted from this development path (Blackdiamond) runs on a windows based PC and provides more or less the same core capability as the real time (OEM 4 based) software but has much more flexibility in terms of available output than the real time system.

The algorithmic base of a large portion of the inertial software used was Kingspad, an inertial software suite developed over the last ten years at the University of Calgary under K.P Schwarz. Although the form of the software as it resides on the OEM 4 is different than that provided by the university, the project could not have succeeded without that knowledge base.

In this paper the authors intend to describe the performance of the system and provide test results that validate performance specification. Furthermore, the authors will describe the architecture of the system, including the main hardware and software system components and how they interact. A detailed description of the inertial measurement processing will be provided, including the alignment process, the process that maintains the inertial system parameters (mechanisation), and the Kalman filtering process. The Kalman filter description will include details of the system dynamics definition, the derivation of the system noise components and the updating methodology.

The Kalman filter experiences modelling errors in the form of a condition called "false observability" that is a result of noise injected into the Kalman filter transition matrix from the IMU measurements. An associated false observability condition occurs when the design matrix is dependent upon a set of system parameters that change during the normal estimation process.

As mentioned previously, test results will be provided and this will be followed by some conclusions and recommendations.

PERFORMANCE SUMMARY

The system performance elements are the quantities that a user is interested in that the system can provide, namely position, velocity, attitude and their associated variance-covariance matrices. In order to quantify the system performance, it is useful to describe it during various scenarios. The factors that must be considered include the

GPS measurement types available currently and previously, and the current state of the system. The scenarios identified include alignment, alignment to steady state in the presence of either single point or differential carrier (RTK) GPS position measurements, and open loop performance after steady state has been achieved. Therefore, the specification is actually quite involved, and so only a subset of them is included here. That subset corresponds to the system performance after it has been through the coarse alignment and RTK measurements have been available while the system has been moving for at least 1 minute. The performance with and without GPS (open loop) is considered.

Table 1: Position Accuracy with GPS

GPS Position Type	Accuracy (1 sigma)
Stand Alone	0.5 to 2 m
Code Differential	0.25 to 1 m
RT-20 (Carrier Float)	0.05 to 1 m
RT-2 (Carrier Fixed Integer)	0.02 m
Post Processed	0.02 to 2 m

Table 2: Velocity And Attitude Accuracy with GPS

Item	Accuracy (1 sigma)
Velocity	0.007 m/sec
Roll	0.013 deg
Pitch	0.013 deg
Azimuth	0.04 deg

OPEN LOOP PERFORMANCE

The AG11 IMU has a gyro drift of 1 degree per hour 1 sigma, and a 1 millig accelerometer bias. The level of these system uncertainties dictate the open loop performance of the AG11 unless some estimates of these parameters can be made. In the NovAtel Inc. both gyro drifts and accelerometer biases are estimated to bring the error level in the system down to a level such that the GPS carrier ambiguities can be reasonably well defined after a GPS outage of 20 seconds. Since the performance of the system is so strongly influenced by the level to which the gyro and accelerometer biases can be estimated, open loop analysis results for both the uncalibrated and calibrated (steady state) systems are included.

For the first 100 seconds of free inertial, the errors take on the characteristics seen in Figure 1 and 2 below. Figure 1 shows the free inertial performance after a good initialization with RTK measurements but with no calibration history to reduce the errors in accelerometer or gyro biases. Figure 2 shows the open loop performance when the system has been well calibrated so that only 10% of the initial accelerometer and gyro biases are unaccounted for. The position errors shown are taken from

[14] and derived from error equations [11][12] that predict the effect of the various components seen on the figures.
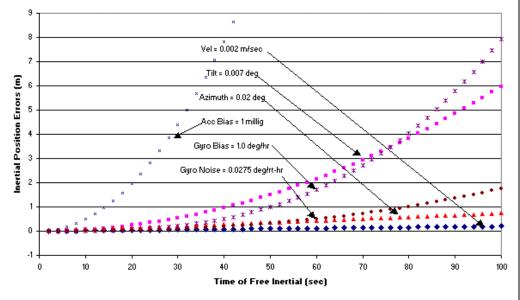
The reason that the open loop performance is important is not only to fulfill its function as a positioning device when GPS is unavailable or degraded, but also so it is accurate enough to successfully reinitialize the RTK filter. The target performance is to be able to reinitialize within 6 seconds, provided the signal outage is less than 5 seconds. This makes the expected accuracy of the integrated position continuously better than 10 cm through momentary GPS outages provided the system is well calibrated.

Fig 1 Open Loop Performance with no calibration

Fig 2 Open Loop Performance with well calibrated system

The following Figure 3 shows the combination of all the deterministic position errors in an RMS plot that compares the calibrated and uncalibrated systems.
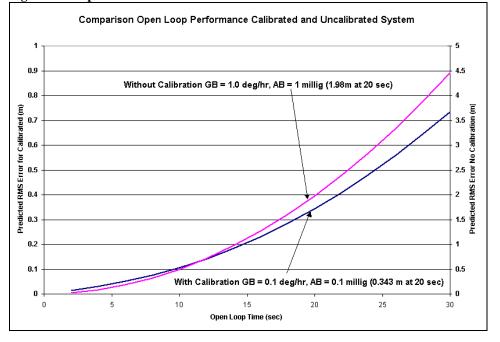
Figure 3 Comparison of Deterministic Error RMS from all sources for calibrated vs Uncalibrated systems

Comparison Open Loop Performance Calibrated and Uncalibrated System

Without Calibration GB = 1.0 deg/hr, AB = 1 millig (1.98m at 20 sec)

With Calibration GB = 0.1 deg/hr, AB = 0.1 millig (0.343 m at 20 sec)

SYSTEM COMPONENTS

The "system" consists of 4 sub-systems, namely the inertial, GPS, data collection and post-mission software sub-systems. The inertial sub-system is a Honeywell HG1700 tactical grade IMU. The GPS sub-system is a NovAtel Inc. OEM4 dual frequency GPS receiver whose software has been modified to process GPS and inertial measurements in a decentralised filter. The data collection sub-system time tags the inertial measurements with a GPS time accurate to 100 microseconds and saves measurements and processed data generated by the GPS sub-system. The post-mission software sub-system has the flexibility to either duplicate the processing carried out by the real time system or to process it in some other way. The post-mission software is also used to pre-test new developments before they are integrated into the real time system.

The Honeywell IMU is a strapdown inertial measuring unit that uses a triad of accelerometers and ring laser gyros mounted orthogonally inside a compact 15 cm high by 15 cm diameter cylindrical case to measure specific forces and angular increments experienced in the units body frame. Internally, delta velocity and delta angles are sampled at 600 Hz. From these, coning and sculling compensations are generated and applied to accumulated delta velocities and angles that we incorporate in our navigation software at a 100 Hz rate. The IMU can be either an AG11 (1 milli-g accelerometer bias, 1 degree/hr gyro drift) or AG17 (3 milli-g accelerometer bias, 10 degree/hr gyro drift). The other system specifications for the two IMU units are the same, and they are included here from [1] because they are related to some of the modelling issues discussed later on.

Table 3: HG1700 AG11 Accelerometer Specifications

Accelerometer Parameters Description	Magnitude
Scale Factor Accuracy (ppm 1 sigma)	300
Scale Factor Linearity (ppm 1 sigma)	500
Bias. Milli-g 1 sigma	1 (AG11)
VRE, micro g's max	500
Axis-Alignment Stability urad 1 sigma	500
Axis-Alignment Stability (non-orthogonality) urad 1 sigma	100
Output noise m/sec	0.0024
Velocity Random walk m/sec/rt-hr max	0.0198

Table 4: HG1700 AG11 Gyro Specifications

Gyro Parameters Description	Magnitude
Scale Factor Accuracy (ppm 1 sigma)	150
Scale Factor Linearity (ppm 1 sigma)	150
Bias. Deg/hr 1 sigma	1 (AG11)
Axis-Alignment Stability urad 1 sigma	500
Axis-Alignment Stability (non-orthogonality) urad 1 sigma	100
Output noise micro/rad	80
Angular Random walk deg/rt-hr max	0.125

The data collection saves measurements and processed data generated by the GPS sub-system.

The post-mission sub-system serves as a development platform for the real time inertial/GPS software. It has much of the functionality of the real time process but none of the cycle time limitations associated with a real time process. So it can produce output records at any rate up to 100 Hz in ASCII or binary that will contain all or any of the inertial system components referenced to one of several available reference frames. There are literally thousands of possible data combinations available to the user.

The GPS sub-system is a NovAtel Inc. OEM 4 dual frequency receiver modified to incorporate inertial measurements in its navigation solution. It can provide L1/L2 range and carrier measurements capable of single point, pseudo range differential and carrier based differential positioning at a 20 Hz rate. When the inertial
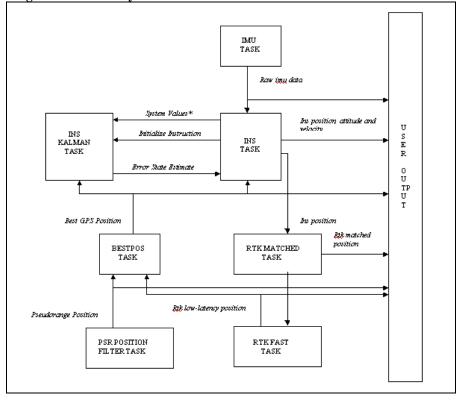
measurements are available it time tags these with a GPS time accurate to 100 microseconds and then uses a decentralised approach to generate a blended GPS/INS solution.

The time synchronisation is quite clever. It depends on a counter within the MINOS4 correlation chip that is slaved to GPS time and has a resolution of 1 micro second. An interrupt service routine with a high priority waits for incoming data on the serial port linked to the HG 1700. When data is sent to the OEM 4 the ISR wakes up when the serial driver makes the first byte available and immediately reads the MINOS 4 counter and uses it to reconstruct the GPS time used to tag the inertial message.

The system software architecture is shown on the following diagram:

Diagram 1 GPS SubSystem Software Architecture

The steady state process is described as follows: The inertial measurements are collected and time tagged in the IMU task. Then they are sent to and processed in the INS task at a 100 Hz rate to generate position, velocity and attitude. These are available for logging to the user, although there is a limitation on the amount of 100 Hz data that can be sent at once (one of raw, position etc.). Every time a 1 second boundary is crossed, an interpolated copy

of the system components is generated. The position is sent to the RTKMATCHED task in case it needs to be used for a once only per resolution floating ambiguity filter initialization. If the system determines it is stationary, it signals to the INS KALMAN task to do a zero velocity update (ZUPT). If not, it waits until a position is available from one of the GPS filter tasks as determined by the BESTPOS task (but originating in either PSR POSITION

FILTER task or RTKFAST task) and uses this position in INS KALMAN task to do a position update. After the update, the state is propagated up to the current time, applied to the system at the current time and reset.

A detailed description of the inertial processing follows.

INERTIAL PROCESSING

The inertial/GPS integration software resides in evolving flavours on both the OEM4 GPS unit as well as on the post-mission software suite. It consists of 4 functional sections, namely a type/frame sensor section, a coarse alignment section, a mechanisation section and a Kalman filter. The type/frame sensor and coarse alignment sections are executed in order during a stationary period at the beginning of every mission. The mechanisation section is executed once every 10 msec, and the Kalman filter section is typically executed once per second, although this can vary depending on the availability of GPS position measurements and ZUPTS.

FRAME DETECTION

Different applications can be satisfied with different grades of IMU, and different users have various installation constraints that make the usual z up, y front, x right body to vehicle frame relationship impossible to satisfy. So the type/frame sensor section has the function of determining the IMU model (AG 11 or AG17) type and of also ensuring that the selected xyz body frame assignment satisfies requirement that the y axis is not parallel to the gravity vector. The knowledge of the model is required to ensure the measurements are scaled correctly, to assign initial uncertainties to the attitude states after the coarse alignment is complete and to assign appropriate entries to the Q matrix during the Kalman filter process. To do this, the software makes the assumption that the system is stationary at start-up and that the model is AG 11. It then takes the ratio of the scaled length of the acceleration vector with the magnitude of normal gravity. Agreement within 20% indicates the model selection is correct, otherwise the system assumes the model is AG 17. The axis assignment (manufacturer's body frame to user body frame) must be made if the IMU is mounted arbitrarily. So before the course alignment starts, the system picks one of six mappings of the manufacturer's body frame to user body frame such that the z axis has the largest positive acceleration magnitude. The type and frame identification takes 5 seconds. Once the IMU type and frame mapping have been determined, the system can initiate a coarse alignment.

COARSE ALIGNMENT

The coarse alignment procedure follows [2] page 198. Given the user position, a triad of orthogonal vectors representing the local level frame can be specified. These vectors consist of the gravity vector, the earth's angular velocity vector and the cross product of the first two. The same vectors transformed to the IMU body frame are measured by the accelerometers and the gyros in the IMU, and the cross product of the acceleration and angular rate vectors. So the 2 sets of three vectors can be concatenated to form 2 matrices S^l and S^b which are related by the transformation

$$S^b = R_l{}^b\, S^l$$
Or
$$(S^b)^T = (S^l)^T\, R_b{}^l$$

Where $R_l{}^b$ is the rotation matrix used to transform a vector from the local level to the body frame, and $R_b{}^l$ is its transpose.

So $R_b{}^l = ((S^l)^T)^{-1}\, (S^b)^T$

Once $R_b{}^l$ is computed, the rotation matrix Rbe used in the system to relate the body frame measurements to the computational (ECEF) frame can be computed via $R_b{}^e = R_b{}^l R_l{}^e$. In addition, the roll, pitch and azimuth elements can be generated from specific elements of the $R_b{}^l$ transformation matrix, for example

Roll = $ArcSin(R_{3,2})$ = $ArcSin(-f_y/g)$
Pitch = $ArcTan(-R_{3,1}, R_{3,3})$ = $ArcTan(f_x/g, -f_z/g)$
Azimuth = $ArcTan((f_x\omega_z - f_z\omega_x)/(\omega g Cos(\varphi)), (\omega f_y Sin(\varphi) + \omega_y g)/(\omega g Cos(\varphi)))$

Where:
f_x, f_y, f_z are specific forces measured in the body frame of the IMU
ω_x, ω_y, ω_z are angular rates measured in the body frame by the IMU
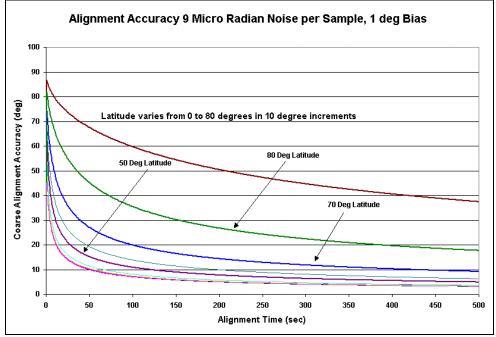ω is earth rotation rate
g is the magnitude of normal gravity
φ is latitude.

After the coarse alignment the attitude accuracy for the AG11 is limited by the accelerometer biases in the case of horizontal alignment to 0.06 degrees and by gyro biases in the case of alignment about the vertical axis (azimuth) to 6 degrees. The AG17 horizontal and vertical axis alignment accuracy is 0.18 degrees and 45 degrees (at latitude 50 degrees). The azimuth is particularly inaccurate because of the high gyro drift to earth rate ratio. The coarse alignment accuracy is limited by the gyro bias uncertainty but improves over time as the ratio of the averaged noise on the accumulated gyro measurements is reduced. This is described by:

$\sigma_{Az} = 57.29577 \; ArcTan((\sigma_b^2 + \eta/t)^{1/2}/(\omega_e Cos(\varphi)))$

Over time, the azimuth uncertainty decreases to its limit as shown in Figure 4 below made for the AG11 case in which the gyro noise (RMS) is 9 micro radians per 10 msec sample and the gyro drift uncertainty is 1 degree per hour.
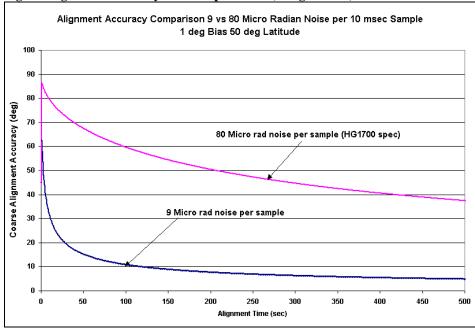
Fig 4: Theoretical Alignment Accuracy (9 Micro Radian Noise per Sample, 1 deg Bias)

It is clear from the equation above used to compute azimuth, that the alignment accuracy over time will be dependent on the noise on the gyros, and in particular on the noise on ω_x when the body frame is aligned horizontally such that ω_x points east. It turns out that the specified noise level on the HG1700 is in many cases very conservative, and in fact the system has a range of measurement noise that varies by a factor of 10. The effect of varying the noise level on this term is shown on Figure 5 below.

Fig 5: Alignment Accuracy Noise Dependence (1 degree bias)

The accuracy of the alignment over time has such a dependence on the level of noise that in order to have something close to an optimal system, the noise level on the measurements must be known and applied. This statistic is measured during the frame determination process, and is used in the estimation of the initial attitude accuracy as well as in the application of process noise during the Kalman filter propagation.

The coarse alignment takes up to 55 seconds, but if the system starts moving before the 55 seconds are up, the software will begin the navigation phase automatically.

In the real time software, the user has the capability at any time, but presumably will only use it when the system isn't moving, to initiate a coarse alignment and this has the function of re-initializing the system parameters as well as restarting the coarse alignment process.

MECHANISATION

Once the coarse alignment is completed, the system has a set of initial conditions that it can combine with the raw IMU measurements to keep the system parameters current. This process is described as the system mechanisation. The function of the mechanisation process is to propagate the inertial system parameters from the ending boundary of the previous measurement interval to the end boundary of the current measurement interval. The parameters include position, velocity and attitude, and the propagation uses the measured delta velocities and delta angles in the solution of the fundamental differential equations:

First
$$dR^e_b/dt = R^e_b(\Omega^b_{ei} + \Omega^b_{ib})$$

Then
$$d^2r^e/dt^2 = R^e_b f^b + g^e - 2 \Omega^e_{ie} dr^e/dt$$

The first equation is solved in order to maintain the attitude relationship between the body and computational frame (in this implementation ECEF). In this process the attitude is maintained as a quaternion, which is somewhat more efficient than a 9 element direction cosine solution, but then that transformation matrix R_b^e has to be recomputed every sampling time from the quaternion elements via:

$$R^e_b = \begin{bmatrix} r_{11} & r_{12} & r_{13} \\ r_{21} & r_{22} & r_{23} \\ r_{31} & r_{32} & r_{33} \end{bmatrix} = \begin{bmatrix} q_1^2 - q_2^2 - q_3^2 + q_4^2 & 2(q_1q_2 - q_3q_4) & 2(q_1q_3 + q_2q_4) \\ 2(q_1q_2 + q_3q_4) & q_2^2 - q_1^2 - q_3^2 + q_4^2 & 2(q_2q_3 - q_1q_4) \\ 2(q_1q_3 - q_2q_4) & 2(q_2q_3 + q_1q_4) & q_3^2 - q_1^2 - q_2^2 + q_4^2 \end{bmatrix}$$

The second equation is solved in order to maintain the system's position and velocity. This 2nd order equation can be used to generate 2 first order equations by introducing the vector v^e to represent velocity in the e-frame.

Then
$$dr^e/dt = v^e$$
$$dv^e/dt = R^e_b f^b + g^e - 2 \Omega^e_{ie} dr^e/dt$$

In the equation for dv^e/dt, the effect of gravity and Coriolis force are removed from the measured specific forces transformed to the ECEF frame via $f^e = R^e_b f^b$. The basic reference for the mechanisation method was [3] and [4].

KALMAN FILTERING

A Kalman filter is a procedure that broadly consists of two steps used to optimally estimate a series of parameters that describe the behaviour of a system. The system in this case is the inertial system and the parameters are those that must be known for the inertial system behaviour to be predictable. The two steps are labelled for the purpose of this paper the propagation step and the update step. The implementation of the two steps presupposes a system description consisting of a set of state variables that describe errors in the system as well as an associated variance covariance matrix that describes the current knowledge level of the state. It also presupposes a set of observational data that can be related to some elements in the state via some kind of functional relationship that can be put into the context of a linear relationship. This section will describe the system, the observation set and its relationship to the system, the propagation, with emphasis on the dynamics and stochastic characteristics of the system, and the updating step. The equations are well known and are repeated here from [6][7] just for easy reference.

Propagation step:

State: $x(-) = \Phi x(+)$
Covariance $P(-) = \Phi P(+)\Phi^T + Q$
where x is the state vector (+) after update, (-) after propagation
P is the state variance covariance matrix
Φ is the transition matrix, the time solution of the dynamics matrix describing the dynamics of the system
Q is the matrix describing the time propagation of the spectral densities of the state elements.

Update step:

$K = P(-)H^T(HP(-)H^T+R)^{-1}$
$x(+) = x(-) + K(z-Hx(-))$
$P(+) = (I-KH)P(-)$
where z is the observation vector
R is the observation variance covariance matrix
H is the linear relationship between the observation and state vector
K is the Kalman gain matrix

The system (modified from [4]) consists of a state vector and its associated covariance matrix. The state represents system errors and has 18 elements, 3 for each of position, velocity, attitude, gyro biases and accelerometer biases and IMU to GPS antenna offsets. The position, velocity and attitude states model errors in the ECEF frame. The bias and offset states model errors in the body frame. Only the filter in the post mission version has been modified to estimate the IMU to GPS antenna offset. The position, velocity, attitude and offset states are modelled as random walks and the bias states are modelled as Gauss-Markov states. The state vector in the Kalman filter is initially assumed to be the zero vector because any error estimates are initially (and in fact after every update) applied to the parameters (position, velocity, attitude and bias terms) that are used to maintain the system in the mechanisation process.

The update step uses the linear relationship between the state and observation vectors in conjunction with the covariance matrices related to those vectors to determine both corrections to the state vector and to the state covariance matrix.

PROPAGATION STEP

The propagation step uses knowledge of the state dynamic behaviour determined from the physics of the system and the stochastic characteristics of the system over time to propagate the state and its covariance from some past time to the current time. The dynamics and stochastic properties of the system are described in more detail in this section.

The dynamics matrix for the modified (18 state) system is the following:

$$F = \begin{bmatrix} 0 & I & 0 & 0 & 0 & 0 \\ N & 2\Omega_{ie}^{e} & F & 0 & R_{b}^{e} & R_{b}^{e}\Omega_{eb}^{b} \\ 0 & 0 & \Omega_{ie}^{e} & R_{b}^{e} & 0 & 0 \\ 0 & 0 & 0 & -\beta_{g} & 0 & 0 \\ 0 & 0 & 0 & 0 & -\beta_{a} & 0 \\ 0 & 0 & 0 & 0 & 0 & 0 \end{bmatrix}$$

The $R_{b}^{e}\Omega_{eb}^{b}$ term is required for the differential equation

$$\delta\dot{v} = \dot{R}_{b}^{e}\delta O^{b} = R_{b}^{e}\Omega_{eb}^{b}\delta O^{b}$$

which links the velocity error rate to error in the body frame offset between the IMU centre and the GPS antenna.
N is the matrix tensor of derivatives the normal gravity vector parameterized in the ECEF frame with respect to position at the user's current position. It links errors in velocity error rate to errors in position.

F is a skew symmetric matrix of specific force elements parameterized in the ECEF frame. These are generated from the raw delta velocity measurements (transformed to the ECEF frame) accumulated over ½ second time intervals, which is the delta time used for the state covariance propagation.

R_{b}^{e} is the rotation matrix that transforms vectors in the body frame to the ECEF frame. So gyro drift states modelling IMU biases are transformed to the ECEF frame and applied directly to the attitude error rates and similarly the accelerometer bias errors are transformed and applied to the velocity error rates.

$(d\delta v/dt)_{e} = R_{e}^{b} d_{a}$ relates the velocity error rate in the ECEF frame to accelerometer biases in the body frame. And the transformation
$(d\varepsilon/dt)_{e} = R_{e}^{b} d_{g}$ relates the attitude error rate in the ECEF frame to gyro biases in the body frame.

β_{g} and β_{a} are time constants of the Gauss-Markov processes which model the gyro and accelerometer bias states respectively. These are derived from the HG1700 accelerometer and gyro random walk characteristics.

The Kalman propagation

$$P(-) = \Phi P(+)\Phi^{T} + Q$$

of the covariance is done once per ½ second because a 1 second delta time led to too much degradation in high dynamic environments. A ½ second propagation makes the assumption of constant coefficients in the dynamics matrix a reasonable one and furthermore allows for a first order solution of that matrix system of differential equations so that $\Phi = I + \Delta t F$ is a reasonable approximation. There is no state propagation because the state is fed back into the system after every update and set to zero. The real time system reduces the computation required in the 2 Hz propagation by only using the non-zero elements of the transition matrix during the P matrix pre and post multiply.

The initial P matrix elements are assigned based on the best knowledge available after the system alignment. This is a function of the system parameters, the type of GPS position available and the quality of the alignment including the time in stationary mode and on the noise level of the IMU measurements used in the alignment.

The Q matrix elements are generated from formulas that incorporate the HG1700 system specifications (either the AG 11 or AG 17 models). The relevant system parameters used to generate Q elements are the accelerometer and gyro scale factor accuracy and linearity, the velocity random walks the angular random walk, accelerometer and gyro output noise. Parameters that have not been accounted for

are vibration rectification error (VRE) for the accelerometers and axis alignment stability for both the accelerometer and gyro axis. The later is a short coming of the system but should not affect the filtering performance provided that the temperature of the unit is stable and provided that the primary output required is position and not attitude.

Accelerometer and gyro noise values in the specification are quite conservative, and the actual noise values measured varies a lot from the specification (by a factor of 10) and a lot between one axis and another (by a factor of 3 or 4). This statistic (noise level) is computed before the alignment (during the type/frame detection portion of the process) and applied to generate the initial alignment precision as well as process noise values for the attitude and velocity states.

The IMU measurement noise η_{acc} and η_{gyro} contributes q values for the position (see [7]), velocity and attitude states follows:

$q_p = (\Delta t^3/3)*10*\eta_{acc}$ (m/sec)^2/sec
$q_{pv} = (\Delta t^2/2)*10*\eta_{acc}$ (m/sec)^2/sec
$q_v = \Delta t*10*\eta_{acc}$ (m/sec)^2/sec
$q_{att} = \Delta t*10*\eta_{gyro}$ (rad/sec)^2/sec

The gyro and accelerometer bias terms are modelled as Gauss-Markov states. The system specifications for the bias terms describe a random walk process. So the two processes are reconciled by trial and error with a starting point for the q specified as:

$q_g = (0.042/57.29577)^2/3600$ (rad/sec)^2/sec
  $=1.469e\text{-}10$ (rad/sec)^2/sec
for the gyro and
$q_g = (0.0198/(3*60))^2$ (m/sec^2)^2/sec
  $=1.211e\text{-}8$ (m/sec^2)^2/sec
The time constant for both of these processes was selected as 4 hours, so $1/\beta = 14400$ seconds.
After some experimentation modified q values of
$q_g = 4.08e\text{-}14$ (rad/sec)^2/sec
and
$q_g = 3.365e\text{-}12$ (m/sec^2)^2/sec
were selected

The velocity and attitude states are modelled as random walks and the basic process noise values applied to these is a function of the noise levels on the accelerometers and gyro measurements respectively. But accelerometer and gyro scaling errors are not modelled as states in the system, and so these also will contribute to the uncertainty of the velocity and attitude states in the presence of acceleration and system rotation. In the case of the accelerometers it is not possible to distinguish the scaling and bias errors while the system is stationary. Therefore, in the presence of

gravity, the vertical axis accelerometer bias becomes observable but part of the bias error is the result of the scaling error that axis will have. So during initialisation, the system retains the average specific forces measured while the first estimates of the accelerometer biases are made. Later, when the system starts to move, the specific forces measured by the accelerometers are differenced from the initial specific forces and these differences are used in the following algorithm that describes how the velocity state covariance is modified to take accelerometer scaling errors into account.

If the system had modelled scaling errors, then the uncertainty in the scaling would propagate to the velocity according to:

$$P(-) = (I+\Delta tF)\ P(+)(I+\Delta tF) + Q$$

where

$$F=\begin{bmatrix} 0 & I & 0 & 0 & 0 & 0 & 0 & 0 \\ N & 2\Omega_{ie}^e & F & 0 & R_b^e & R_b^e\Omega_{eb}^b & R_b^eF_\Delta & 0 \\ 0 & 0 & \Omega_{ie}^e & R_b^e & 0 & 0 & 0 & R_b^e\Omega_{eb}^b \\ 0 & 0 & 0 & -\beta_g & 0 & 0 & 0 & 0 \\ 0 & 0 & 0 & 0 & -\beta_a & 0 & 0 & 0 \\ 0 & 0 & 0 & 0 & 0 & 0 & 0 & 0 \\ 0 & 0 & 0 & 0 & 0 & 0 & 0 & 0 \\ 0 & 0 & 0 & 0 & 0 & 0 & 0 & 0 \end{bmatrix}$$

Then the propagation will increase the uncertainty on the velocity states according to

$$P_v(-) = \Delta tR_b{}^eF_\Delta P_{sa}(+)F_\Delta{}^TR_e{}^b$$

Where F_Δ is the diagonal matrix of specific force differences and P_{sa} is the scale factor uncertainty, a diagonal matrix which doesn't change since there is no scale factor estimation. For this the HG1700 specification of accuracy and linearity is combined to give the diagonal elements of $P_{sa} = \sigma_{sa}^2 = (583/1,000,000)^2$.

Therefore every propagation,

$$Q_v = \Delta t\sigma_{sa}^2R_b{}^eF_\Delta\ F_\Delta{}^TR_e{}^b$$

is applied to the velocity state elements of the P matrix.

The gyro scaling errors affect the attitude states in a similar manner, and based on the missing state propagation of gyro scale factor uncertainty to attitude uncertainty, the following Q_a is applied to the attitude state covariance:

$$Q_a = \Delta t\sigma_{sg}^2R_b{}^e\Omega_{eb}{}^b{}_\Delta\ \Omega_{be}{}^bR_e{}^b$$

where
$\sigma_{sg} = 212/1000000$ is the manufacturer's gyro scaling specification combining accuracy and linearity terms,
Ω_{eb}^{b} is the skew symmetric matrix of the instantaneous rotation of the ECEF frame with respect to the body frame parameterized in the body frame.

This completes the description of the Kalman filter propagation step.

UPDATE STEP

The measurements in the decentralised approach are either GPS antenna position or velocity in the case of the ZUPT measurement. In this case, some of the state elements (position and velocity) are observed directly by the GPS or ZUPT observations.
In the velocity update case, the H matrix for the update is
$H = [0,I,0,0,0,0]$,
and in the position update case it is
$H = [I,0,0,0,0,R_{b}^{e}]$

The velocity update is triggered when a set of conditions based on the IMU measurements are met. First, the averaged measured acceleration vector magnitude difference from the magnitude of the gravity vector has to be within a threshold. Second the averaged measured angular rate vector magnitude has to be below a threshold. Then a ZUPT is initiated with an observation covariance based on the thresholds used to detect the stationary condition the first place.

The position update takes place when the GPS filter provides a position and associated covariance matrix. Not including some of the transient position types, there are 4 different position types [8][9][10] all with different accuracies and different time correlated errors with different time constants. These are summarized in the following table along with the expected accuracy, predominant error source and rough correlation time constant.

Table 5: GPS Measurement Error Characteristics

Type	Accuracy (m)	Time Constant	Error source
Single Point PSR	3	5 min	Iono/MP (PSR)
Differential PSR	1	3 min	MP PSR
Carrier Float	1 to 0.20	3 min	MP/Conv
Carrier Fixed	0.02	3 min	MP (car)

The multipath error (MP) related time constants are reduced significantly when the system is moving, down to about 5 seconds except for the carrier float solution type which has time correlated errors as a result of ambiguity

convergence errors. The pseudo range filters don't increase the measurement correlation in of themselves because they are single epoch least squares filters, rather than Kalman filters with some time history from clock rate or velocity states. The carrier fixed position type also has long time constant errors associated with carrier multipath, but the amplitude of these errors is small enough so they can be ignored. Time correlated measurement noise generates a modelling error in the filter if it is not taken into account. One way to do this is to add additional states to the filter which are used to estimate the slowly varying correlation error, but in a real time system additional states risk increasing the computational burden too much. Instead, the measurements are de-weighted for 9 out of 10 observations when the system is stationary or if the system is in carrier float mode. Otherwise, the covariance matrices provided by the GPS position filters are used directly in the Kalman update.

In many environments, the system experiences severe multipath errors (urban canyons are one example where the predominant or even only signal may be a reflected one). To prevent the positions generated with these from corrupting the inertial system parameters via the Kalman update, a six sigma bound is placed on the innovation before it is used to update the filter.

This completes the description of the Kalman filter update step.

MODELLING ISSUES

The Kalman filter is subject to modelling errors that occur when some significant error source has either been misrepresented or even ignored by the filter designer. Typically these are corrected by modifying the state vector and its associated dynamics matrix or by modifying the Q matrix by adding additional system noise. Two modelling errors that occurred during this development had nothing to do with incorrect modelling of the states, but instead were dependent on the generation of the transition matrix Φ and the design matrix H. We call this "false observability", and will show that it is the result of IMU measurement noise in the transition induced case and on coincident state convergence in the design matrix case.

Let's look at the transition matrix generation first. The transition matrix is generated as a solution of the dynamics matrix F vis a vis $\Phi = \Delta t \, F$. Subsequently, the P matrix is propagated according to $P(-) = (I+\Delta tF) \, P(+)(I+\Delta tF) + Q$. Then, during the update, the gain matrix is generated via
$K = P(-)H^{T}(HP(-)H^{T}+R)^{-1}$
In this implementation H is a 3 by 18 matrix which is zero except for the first and last three columns that are the identity and the R_{b}^{e} matrix respectively. So in order for the gains to be non-zero, the off-diagonal terms in the first

three rows of the P matrix must be non-zero. In order to simplify the argument, assume that the system is perfectly aligned to the local level frame at the equator on the Greenwich meridian, so the body, ECEF and local level axis parallel. Assume further that the IMU and antenna are co-located so that no offset sates need be estimated, and finally that the position is known so that position states aren't estimated. Finally, assume the earth has stopped rotating. Then ask the question, "If the system is stationary, what is observable via a velocity update?".

Under these assumptions $R^e_b = R^l_b = I$ and the specific force vector representation in the body, ECEF and local level frame is $f = [0,0,g]^T$. Based on this scenario, the system of differential equations describing the changes of the error states over time is:

$$
\begin{bmatrix} \dot{\delta v} \\ \dot{\varepsilon} \\ \dot{b} \\ \dot{d} \end{bmatrix} = \begin{bmatrix} 0 & F & 0 & R \\ 0 & 0 & R & 0 \\ 0 & 0 & 0 & 0 \\ 0 & 0 & 0 & 0 \end{bmatrix} \begin{bmatrix} \delta v \\ \varepsilon \\ b \\ d \end{bmatrix}
$$

So the transition matrix related to the dynamic matrix will be (for dt = 1.0)

$$
\Phi = \begin{bmatrix} I & F & 0 & R \\ 0 & I & R & 0 \\ 0 & 0 & I & 0 \\ 0 & 0 & 0 & I \end{bmatrix}
$$

and if the velocities are directly observable, the observation matrix H will be

$$ H = [I,0,0,0]^T $$

The criteria that must be satisfied if all 12 of the states in the given system are observable is that the matrix

$$ \Xi = [\ H^T \mid \Phi^T H^T \mid \Phi^{T2} H^T \mid \Phi^{T3} H^T] $$

must be full rank [6]. Expanding Ξ based on the system transition matrix gives

$$
\Xi = \begin{bmatrix} I & I & I & I \\ 0 & F^T & 2F^T & 3F^T \\ 0 & 0 & R^T F^T & 2R^T F^T \\ 0 & R^T & 2R^T & 3R^T \end{bmatrix}
$$

From this it is clear that there are elements in the system that are not observable as long as the transition matrix is constant because the linear combination of columns $C_4 + C_2 - 2C_3$ gives the column $[0]_{12 \times 1}$, which indicates the matrix Ξ does not have full rank.

If the system moves (accelerates and rotates), the columns are no longer linearly dependent, and all the elements in the state become observable to some degree or another. But if the system is stationary, the system attitude accuracy is limited by the uncertainties in the gyro and accelerometer biases. If the uncertainties in the biases were not limited, then the observability matrix shows that the system alignment could never be useful if the system is stationary.

The problem that this theoretical analysis uncovers is that the attitude variance estimate after a coarse and fine (Kalman filter) alignment is much smaller than the theory indicates it should be. The azimuth error during the alignment is mainly influenced by the noise on the angular measurements and by the bias on the gyro. The equation linking these three elements is:

$$ \sigma_{Az} = 57.29577\ ArcTan((\sigma_b^2 + \eta/t)^{1/2}/(\omega_e Cos(\varphi))) $$

Where σ_b is the gyro bias in rad/sec
ω_e is the earth rate in rad/sec
φ is the latitude
η is the random walk error for 1 second
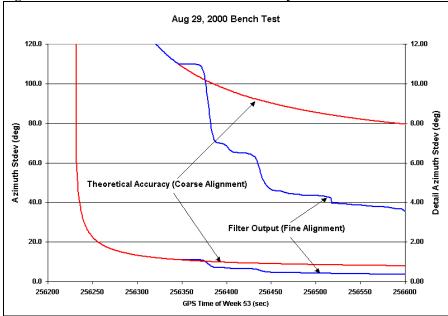
The limit of this expression as t increases without bound is

$$ \sigma_{Az} = 57.29577\ ArcTan(\sigma_b/(\omega_e Cos(\varphi))) $$

that for a bias of 1 degree per hour and a latitude of 51 degrees is 6.0 degrees.

The following figure shows the decrease in the azimuth standard deviation for a stationary system resting on the bench. The theoretical accuracy estimate for the azimuth is also plotted. The accuracy estimate for the azimuth is generated from the Kalman filter state covariance matrix.
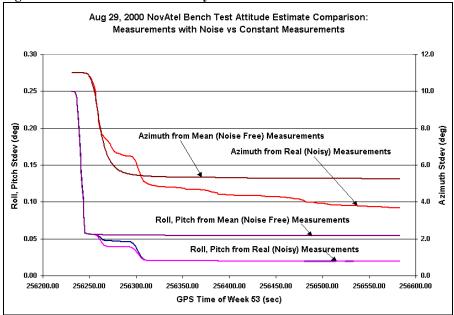
Figure 6 Theoretical vs Filtered Azimuth Accuracy Estimate

Now the theoretical uncertainty limit of 6.0 degrees is much larger than the 3.6 degrees which the filter has determined. One could argue that the reason the filter has so much more success is because the gyro drift elements are estimated in the filter, so the element σ_b is decreasing so the azimuth uncertainty is also decreasing. But, it turns out that the real reason the estimated accuracy is decreasing is that the noise level on the element of F in the dynamics matrix F makes that sub-matrix non-constant even when the system is stationary. This can be verified by computing the average observation on a 10 msec interval based on the entire data

set and using this ideal and constant set of delta velocities and delta angles as inputs to the mechanization equations in place of the measured values. The signal portion of the original measurements (gravity and earth rate) is identical to the constant set, but the constant set has no measurement noise. The only difference between the mean value measurements and the real ones is system noise on the real measurements. The standard deviations of the system state parameters related to attitude, gyro and accelerometer biases are shown on the following plots.

Figure 7 Filtered Azimuth Accuracy Estimate with and without noise on F elements
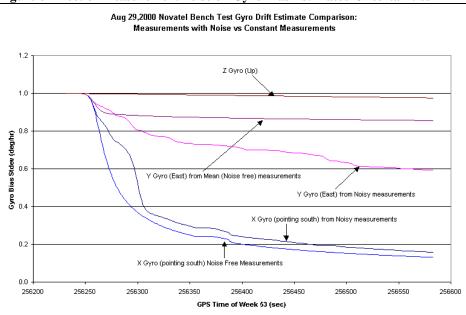
The attitude comparison, shown above, shows that the limiting azimuth standard deviation for the noise free case is 5.25 degrees compared to a final azimuth error estimate of 3.68 degrees for the real measurement case. The 5.25 degrees is more precise than the theoretical limit of 6.0 degrees. The reason this happens is that the horizontal gyro biases are indeed slightly observable, so the standard deviation of the "east" gyro (see note 1 below) is slightly smaller than 1 degree per hour. The steady state "east" gyro bias uncertainty (see plot below) of 0.855 degrees per hour causes a convergent azimuth error uncertainty of 5.17 degrees which agrees closely with the attitude (from mean) error uncertainty seen in the plot above.

A secondary observation related to this discussion is the accuracy of the "north" gyro drift error is clearly observable

and in fact the x gyro drift uncertainty approaches 0.15 degrees per hour. The "east" gyro is not observable because an "east" gyro bias will have the same effect over time on a "north" axis accelerometer as an azimuth misalignment. If after 300 seconds or so of "north" gyro bias estimation, the IMU is rotated 90 degrees so the gyro uncertainty is now predominantly in the north direction rather than east, then the stationary alignment could continue and in the end generate a steady state azimuth error of 0.91 degrees.

Note 1: The gyro drift is associated with the body rather than the local level frame but the y gyro in the body frame coincidentally points east but even if it didn't, there would be a composite "east" gyro whose accuracy impacts directly on the azimuth accuracy because the effect of both of these errors on the "north" accelerometer axis is identical.

Figure 8 Effect of Measurement noise on Gyro Bias Estimated Uncertainties

The pitch and roll accuracies are identical in both the real data case (0.02 degrees after 85 seconds) and the mean data case (0.055 degrees after 30 seconds). The horizontal accelerometer biases cause identical acceleration errors while the system is stationary as do horizontal attitude errors. This is described by the equation:
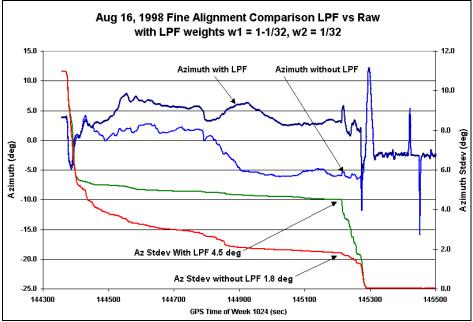
$$e = ArcSin(b/g)$$

This indicates that an accelerometer bias of 1 millig should produce a roll or pitch error of 0.057 degrees. This agrees closely with the horizontal accuracy of both the roll and pitch of the mean observation system (0.055 degrees), and this corresponds even more closely with the steady state estimated accelerometer bias of 0.00949 m/sec^2. The roll

and pitch accuracy of the real (noisy) observation system is far more optimistic at 0.02 degrees.

The problem of transition matrix false observability can be alleviated to a certain degree by averaging the specific force observations used to generate the *F* sub-matrix of the F matrix. When this low pass filtering is put in place, the standard deviation of the azimuth, after a long stationary alignment reaches a steady state of between 4.5 and 5 degrees rather than the typical unfiltered steady state value of between 1.5 and 2 degrees. This is demonstrated in Figure 9 below that compares the fine alignment process with and without a low pass filter on the raw measurements while the system is stationary.

Figure 9 Effect of Low Pass Filtering to remove Measurement noise

The second case of false observability occurs because in the H matrix, there is a component R_b^e that rotates the estimated IMU to antenna offset from the body to the ECEF frame. During convergence, and depending on the quality of the coarse alignment, the azimuth component of the R_b^e matrix can vary by as much as 50 degrees. This causes the gain elements related to the normally unobservable portions of the offset states to become non-zero and a resulting reduction in the variance of the offset elements in the P matrix. As a result, when the system actually does start to move, the offset vector is slow to converge and often to the wrong value. This is a variation of the problem in an extended Kalman filter (see [7] for example) in which errors in the trajectory generates errors in the H matrix that cause 2nd order state errors. The approach used to solve this problem is to use the same initially defined R_b^e matrix throughout the static portion of the fine alignment. Then the theoretically unobservable portions of the offset states remain unobservable until the system starts to move and the associated rotation is reflected in the P matrix off-diagonal terms, which correctly allows the offset state elements to become observable.

TEST RESULTS

There are results from 3 tests presented in this paper. The first set of test results provided is intended to show that the position provided by the integrated solution satisfies the requirement that the position error follows the curve of the deterministic error shown on Figure 3, and that the standard deviations for the open loop position represent the errors reasonably well. The second set of test results is intended to demonstrate the improvement the integrated system has

over a stand alone GPS receiver in the time it takes to fix integer ambiguities. Finally, a third set of test results is intended to give a qualitative measure of the system's navigation capability through some of Calgary's urban canyons.

The rate of error growth in the absence of GPS measurement updates is shown on Figure 10 and 11 below. These were generated off line by the Blackdiamond post mission software. The data was collected north of Calgary near Balzac on August 12, 1999. The route selected was an inverted "L" shaped baseline which went north roughly 5.5 km., then east the same distance. The satellite coverage was very good, and in fact there were only 200 seconds out of about 4500 that did not have RTK GPS positions. Two runs with stops every 3 minutes were made and the driving speed was 100 km/hr. The open loop accuracy is seen by comparing the inertial positions with the GPS RTK positions in places where GPS is not used to update the system. Since the coverage was uniformly good, the system had to be artificially restricted from using the available GPS positions. The behaviour of the calibrated system was more interesting, so the open loop data was taken once the system had estimated its biases. This occurred about 1000 seconds after the system began to move at 145285, but the open loop test wasn't initiated until 146860 because that was the last time RTK was unavailable. On intervals of 120 seconds after that time, 20 seconds of position measurements provided by the OEM4 are used to generate misclosures but these are is not used to update the system. The position misclosures show the error in the free inertial system, and the standard deviations show the expected

position error in the system. The misclosures and standard deviations have been transformed to the local level frame.
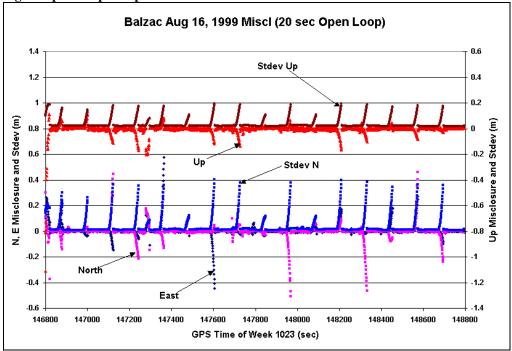
Fig 10 Open Loop INS position difference with GPS RTK

The Figure 11 shows a detail of a typical set of open loop position errors. The errors are well represented by the reported standard deviations, and those are very close to the predicted 1 sigma errors for a well calibrated system seen above on Figure 3.
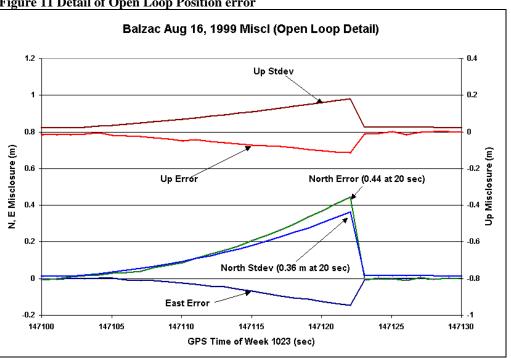
Figure 11 Detail of Open Loop Position error

The following plot shows a comparison of the position consistency of the combined INS/GPS system and a GPS only system. The GPS and the combined system are independent except they are processing signals taken from the same antenna. Both GPS units are operating in single point mode. When less than 4 satellites are available, no GPS position is shown. The data was collected in the urban canyons of downtown Calgary. The buildings in the area range in height between 20 to 70 storys and are often joined by elevated pedestrian walkways which further obstruct the satellite coverage. This is evidenced by the long intervals with no GPS position availability.
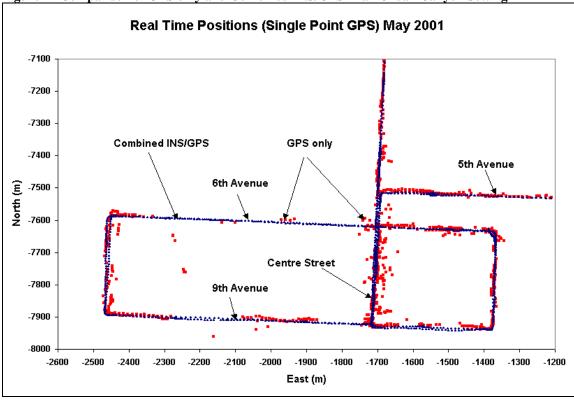
Figure 12 Comparison of GPS only and Combined INS/GPS in an Urban Canyon Setting

A major functional requirement for this system is the proposed capability of the combined filter to provide enough information to the GPS RTK filter to help it resolve ambiguities quickly and reliably. Preliminary tests over the last 6 months have shown this is possible provided the GPS signal blockage is not too long. A test conducted for the purpose of this paper demostrates the enhanced resolution capability that the integrated system has. The test was carried out on the Deerfoot trail, a major north south freeway just east of the NovAtel Inc. office. The test equipment included the integrated OEM4INS system and a standard OEM4 in the test van and an OEM4 base station on a known point, plus radios capable of transmitting the RTK base observations to the van over a distance of about 2 kilometres. Both GPS receivers in the test van were connected via splitters to both the GPS antenna and the differential serial line from the radio.

The portion of the Deerfoot trail used has two overpasses spaced less than 2 km apart. The procedure used was to collect the data while driving in a loop south on the west lane under the south overpass, north on the east lane and under the overpass and repeat many times. The difference in position standard deviation between the OEM4INS combined solution and the control GPS only standard OEM4 solution shown in Figure 12 shows the effectiveness of the OEM4INS system in not only maintaining very good accuracy throughout periods of brief obstructions but also in helping the RTK filter in the combined system to resolve ambiguities. The combined resolutions were verified to be correct by comparing those resolved position with those of the control OEM4 receiver once the resolutions had been made there. The combined system took 250 seconds to initialize after start up, but after that time the height standard deviation was always less than 0.12 metres. During the same period (1954 seconds including 12 passes under one overpass or the other), the standard OEM4 had a height standard deviation of 0.30 metres or more for 891 seconds or 45% of the time. The following graph shows the standard deviation comparison over time. Note that the

combined system has a scale (left hand side) which is 100 times smaller that the scale for the GPS only height
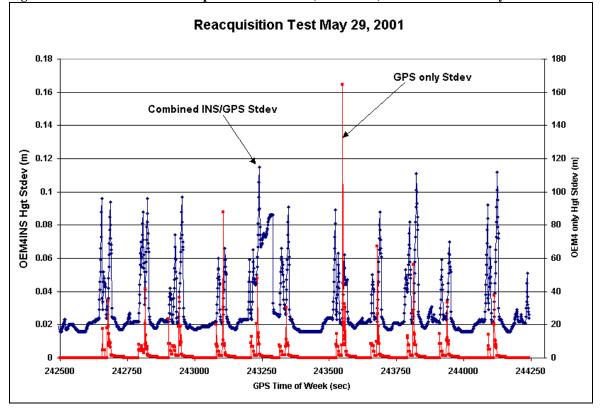
standard deviation.

Figure 13 Standard deviation comparison Combined (OEM4INS) and OEM4 GPS only

CONCLUSIONS AND RECOMMENDATIONS

Based on this paper, a number of conclusions can be made:

1) The HG1700 models AG11 and AG17 have been successfully integrated onto the NovAtel Inc.OEM4 GPS receiver.

2) To achieve this, a decentralized filter architecture was adopted. The major components include the various GPS (pseudo range and RTK) filters and the INS filter.

3) Position update information is provided to the INS filter from the best position available from the GPS filters. Some deweighting is used in certain circumstances to reduce the effect of correlated measurement noise on postion measurements used to update the INS filter.

4) Position information from the INS filter is used to provide a once per resolution initialization to the floating ambiguity portion of the RTK filter.

5) The OEM4INS system can use either an AG11 or AG17 model of the HG1700. The system detects which model of inertial system it is linked to and adapts itself accordingly by varying both the scaling of the

measurements, the initial state accuracy estimates and the levels of system noise.

6) The OEM4INS system includes a frame detection component to ensure the y axis of the body frame is not aligned with the gravity vector.

7) The observability of the initial azimuth component of the attitude is very dependent on the level of INS measurement noise, and this varies significantly between different IMUs and from the specification. In order for a reasonable estimate of the accuracy of the initial alignment to be made, noise level estimates are made while the system is stationary prior to the coarse alignment process.

8) A condition called "false observability" causes the azimuth standard deviation to be smaller than it should is a result of noise on the inertial measurements. This is aleviated by low pass filtering the measurements while the system is stationary.

9) A secondary false observability condition affecting the estimation of the antenna offset is the result of convergence of the attitude state and its changing effect on the measurement model. The solution to this problem is to fix the body to ECEF rotation matrix

used in the measurement model until the system starts to move.

10) System noise is added according to both the component specifications (documented and measured) of the HG1700 and the dynamic enviroment the system is in.

11) The position accuracy measured during testing closely reflects the predicted accuracy resulting from the error analysis of the system that is the foundation of the system specification.

12) There are certain measures of success which have been verified directly, while other measures have been verified only indirectly. The improved position accuracy of the system over a stand alone GPS receiver has been verified directly as has the system's capability to significantly reduce the resolution time. The measures which have been verified only indirectly are the systems capability to estimate other system parameters such as velocity and attitude which are also of potential interest our clients in the navigation community, and also parameters such as accelerometer and gyro biases which may not be of any interest to our clients, but will be of importance to getting optimal performance out of the HG1700.

Based on the paper, number of recommendations can be made:

1) The other system components besides position need to be verified. This will be done with a comparison with a more accurate inertial system

2) Features under development, such as the offset estimation function need to be implemented on the real time platform.

3) Almost all the testing to date has been done with the AG11 model of the HG1700. More qualification has to be done with the AG17 model.

ACKNOWLEDGEMENTS

REFERENCES

[1] Military Avionics Division Honeywell Inc., "Specification No. DS34468-01"

[2] K. Britting, **Inertial Navigation Systems Analysis**, John Wiley and Sons Inc 1971.

[3] K.P. Schwarz, M. Wei, "INS/GPS Integration for Geodetic Applications (partial lecture notes for ENGO 623)" , Dept. of Geomatics Engineering The University of Calgary, Jan. 1997

[4] Dr. K.P. Schwarz, Hugh Martell, Dr. Ming Wei, Dr. Naser El-Sheimy, Dr. John Zhang, Dr. Ziewn Liu, Dr. Ahmed Mohamed, Dr. Jan Skloud, Dr. Craig Glennie, Dr. Alex Bruton, "KINGSPAD Source code", University of Calgary, 1999.

[5] G. Siouris, Aerospace Avionics Systems: A Modern Synthesis", Academic Press Inc. 1993

[6] A. Gelb et al, **Applied Optimal Estimation**, M.I.T Press, 1974

[7] R.G. Brown, P. Hwang, **Introduction to Random Signals and Applied Kalman Filtering 2nd Edition**, John Wiley & Sons Inc, 1983

[8] Ford, T.J. and J. Neumann , NovAtel's RT20 - "A Real Time Floating Ambiguity Positioning System", Proceedings of ION GPS '94, Salt Lake City, Utah, Sept. 20-23, 1994, The Institute of Navigation, Washington, D.C. pp. 1067.

[9] J. Neumann, A. Manz, T. Ford, O. Mulyk, "Test Results from a New 2 cm Real Time Kinematic GPS Positioning System", Proceedings of ION GPS '96, Kansas City, Mo., Sept. 17-20, 1996, The Institute of Navigation, Washington, D.C. pp. 183

[10] NovAtel Inc. Document OM-20000046 OEM4 Users Manual

[11] M. Kayton, W. Fried, **Avionics Navigation Systems**, John Wiley and Sons, New Yory, 1997

[12] J. Huddle, "Inertial Navigation System Error Model Considerations in Kalman Filtering Applications", Control and Dynamic Systems, Vol. 20 Academic Press 1983.

[13] I. Williamson, Private conversation, NovAtel Inc, May 28, 2001

[14] T. Ford, "Specification of Performance of the OEM4/HG1700 (AG11) Integrated System (Preliminary)", NovAtel Inc. internal document D03011 Rev. A, Sept. 2000